SAS Honors Seminar 256:
Extraterrestrial Life

10/20/2011

Mid-term project data

Option # 1 – sent

Option # 2 – sent

Option # 3 – coming soon!

Reading for Tuesday (10/25)

Bennett & Shostak 7.3, 9.1-9.2 – possibility of life on Europa, as well as the other moons of Jupiter

articles from the Planetary Report (1999-2007) – oceans on satellites of the giant planets

Pappalardo (2011) – presentation from a meeting taking place this week about a possible future NASA mission to Europa (don't print this out unless you really want to...)

Reading for Thursday (10/27)

Bennett & Shostak 9.3 – possibility of life on Titan, as well as the other moons of Saturn, Uranus, and Neptune

articles from the Planetary Report (2005-2008) – the Cassini/Huygens mission to Saturn and Titan

Schneider et al. (2009) – possibility of an ocean on Enceladus

Klotz (2011) – latest prospects for a Titan balloon mission

Lorenz (2008) – detailed discussion of Titan balloon mission [skim only]

1996 undergraduate research project

http://www.lpi.usra.edu/publications/newsletters/lpib/lpib79/intern79.html

ANNE TAUNTON, University of Arkansas

Advisor: David S. McKay, Johnson Space Center

"SEM Studies of Microbes." A major goal of the exploration of Mars is to determine whether life has developed there. To help understand how potential martian life may have evolved and whether such life might still exist in extreme environments on Mars, we will study selected samples from extreme environments on Earth. Samples of microbes are known to grow in rocks in Antarctica, in hot springs, in highly saline evaporate lakes, in arid deserts on rock surfaces, and deep in the Earth in rocks at depths of 10 kilometers or more. The intern will study representative samples of each of these materials with the scanning electron microscope (possibly supplemented by TEM studies of selected samples) to characterize the morphology and chemistry of the microbes, document the microbe-mineral interactions, and determine the types of fossil preservation, if any. Using published data and papers, the intern will also make a parallel evaluation of Mars environments in terms of their potential to sustain microbial life.

McKay et al. (1996) figure 1

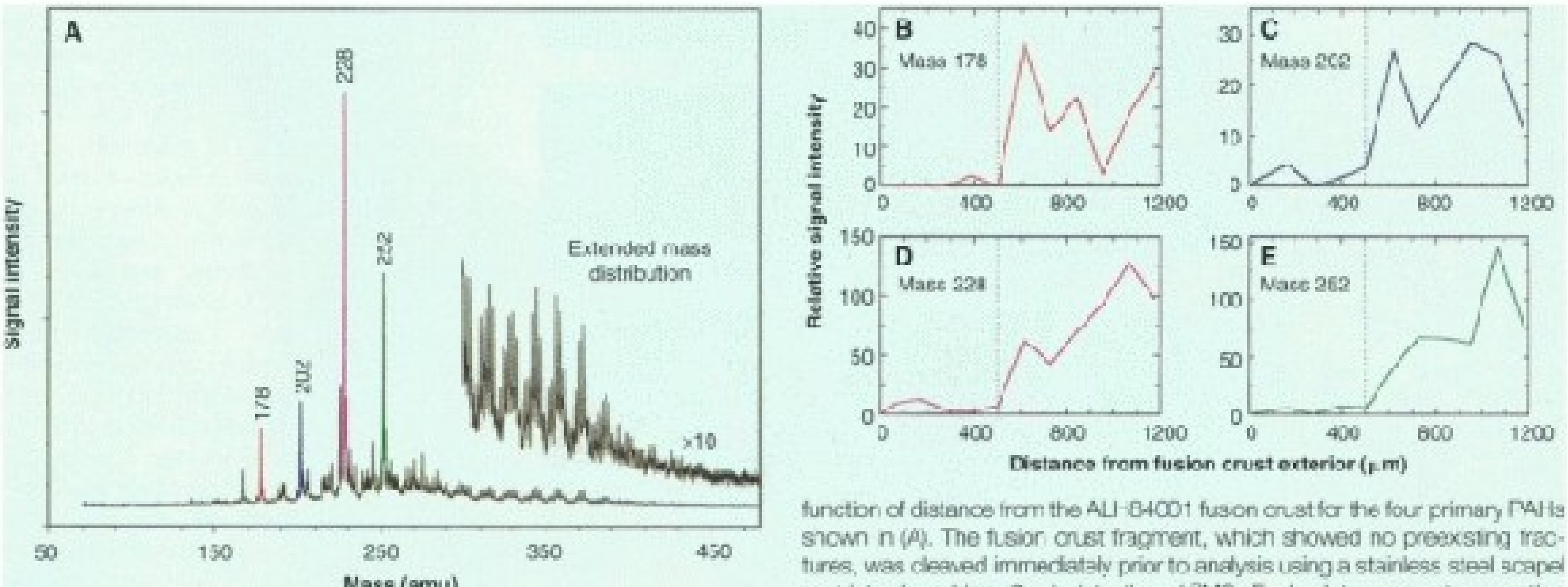

Fig. 1. (**A**) Averaged mass spectrum of an interior, carbonate-rich, fracture surface of ALH84001. The spectrum represents the average of 1230 individual spectra defining an analyzed surface region of 750 by 750 μm mapped at a spatial resolution of 50 by 50 μm. (**B** through **E**) PAH Signal intensity as a function of distance from the ALH84001 fusion crust for the four primary PAHs shown in (*A*). The fusion crust fragment, which showed no preexisting fractures, was cleaved immediately prior to analysis using a stainless steel scapel and introduced in <2 min into the μL[2]MS. Each plot represents a section perpendicular to the fusion crust surface, which starts at the exterior and extends a distance of 1200 μm inward. The spatial resolution is 100 μm along the section line and is the average of a 2 by 2 array of 50 by 50 μm analyses, with each analysis spot being the summed average of 5 time-of-fight spectra.

McKay et al. (1996) figure 2

Fig. 2. False-color backscatter electron (BSE) image of fractured surface of a chip from ALH84001 meteorite showing distribution of the carbonate globules. Orthopyroxene is green and the carbonate globules are orange. Surrounding the Mg-carbonate are a black rim (magnesite) and a white, Fe-rich rim. Scale bar is 0.1 mm. [False color produced by C. Schwandt]

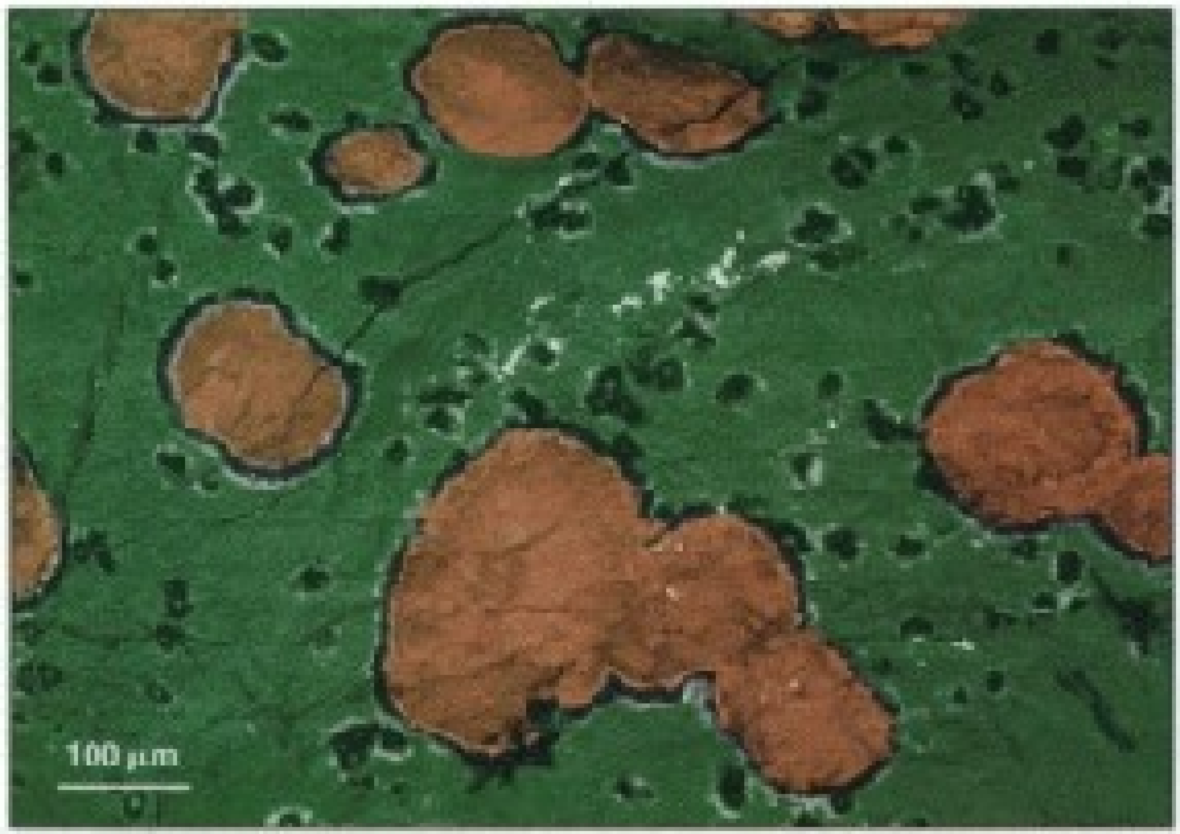

McKay et al. (1996) figure 3

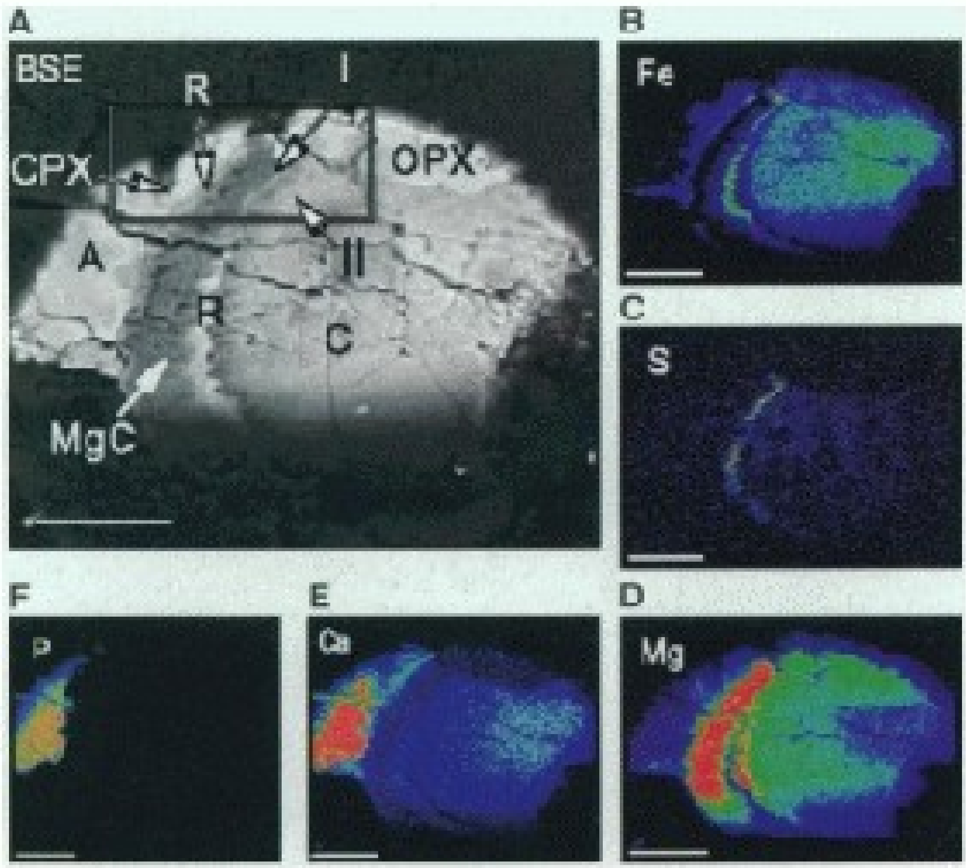

Fig. 3. BSE image and electron microprobe maps showing the concentration of five elements in a carbonate from ALH84001. The element maps show that the carbonate is chemically zoned. Colors range through red, green, light blue, and deep blue, reflecting the highest to lowest element concentrations. Scale bars for all images are 20 μm. **(A)** BSE image showing location of orthopyroxene (OPX), clinopyroxene (CPX), apatite (A), and carbonate (MgC, C). Iron-rich rims (R) separate the center of the carbonate (C) from a Mg-rich carbonate (MgC) rim. Region in the box is described in Figs. 5 and 6. **(B)** Iron is most abundant in the parallel rims, ~3 μm across, and in a region of the carbonate ~20 μm in size. **(C)** Highest S is associated with an Fe-rich rim; it is not homogeneously distributed, but rather located in discrete regions or hot spots in the rim. A lower S abundance is present throughout the globule in patchy areas. **(D)** Higher concentrations of Mg are shown in the Fe-poor outer region of the carbonate. A Mg-rich region (MgC), ~6 μm across, is located between the two Fe-rich rims. **(E)** Ca-rich regions are associated with the apatite, the Fe-rich core of the carbonate, and the clinopyroxene. **(F)** P-rich regions are associated with the apatite.

McKay et al. (1996) figure 4

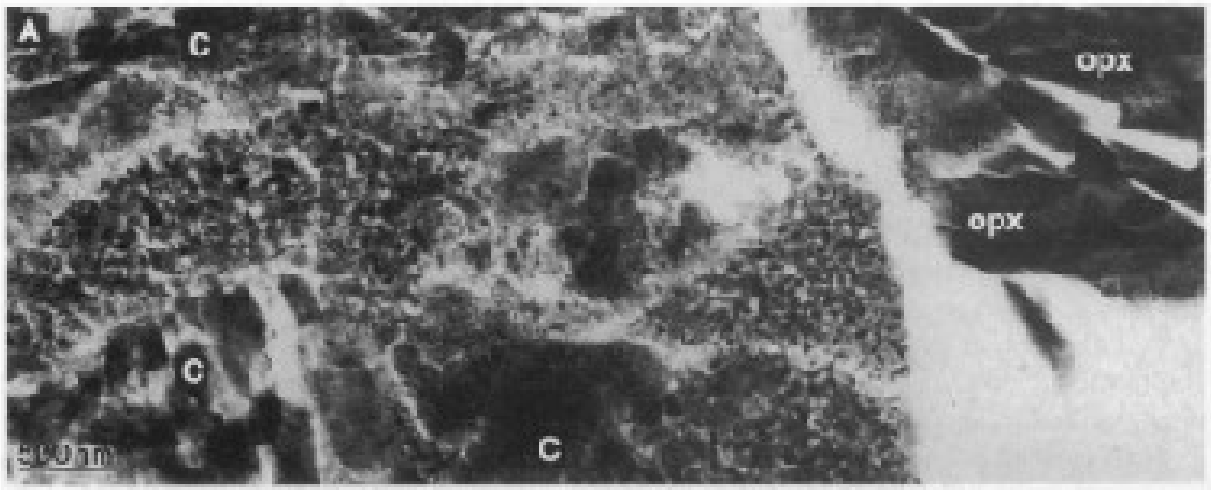

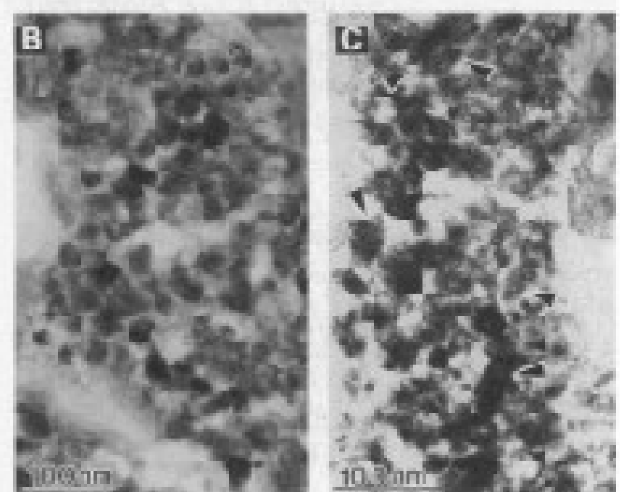

Fig. 4. TEM images of a thin section obtained from part of the same fragment shown in Fig. 3A (from the region of arrow I, Fig. 3A). (**A**) Image at low magnification showing the Fe-rich rim containing fine-grain magnetite and Fe-sulfide phases and their association with the surrounding carbonate (C) and orthopyroxene (opx). (**B**) High magnification of a magnetite-rich area in (A) showing the distribution of individual magnetite crystals (high contrast) within the fine-grain carbonate (low contrast). (**C**) High magnification of a pyrrhotite-rich region showing the distribution of individual pyrrhotite particles (two black arrows in the center) together with magnetite (other arrows) within the fine-grained carbonate (low contrast).

McKay et al. (1996) figure 5

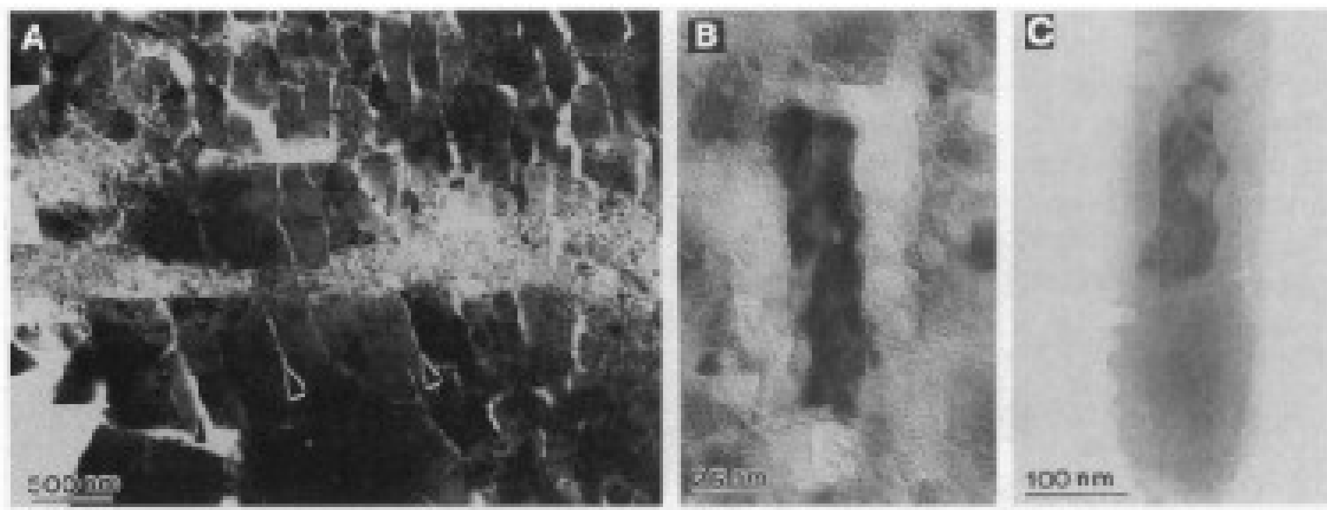

Fig. 5. TEM images of a thin section showing the morphology of the Fe-sulfide phases present in ALH84001 and a terrestrial soil sample. Iron sulfide phase (greigite?—Fe_3S_4) is located in a magnetite-poor region separate and distinct from the magnetite-rich rims (Fig. 3A, arrow II). (**A**) TEM of a thin section showing a cross section of a single carbonate crystal (large black regions; the apparent cleavage features are due to knife damage by ultramicrotomy). A vein of fine-grained carbonate (light gray) is observed within the large carbonate crystal. Possibly greigite and secondary magnetite (fine dark crystals) have been precipitated in this fine-grained matrix. There is a direct relation between the presence of carbonate dissolution and the concentration of the fine-grained magnetite and Fe-sulfide phases. This region shows fewer Fe-rich particles, while regions shown in Fig. 4 contain abundant Fe-rich particles. The cleavage surface of the carbonate crystal does not show any dissolution features (arrows); there is no evidence of structural selective dissolution of carbonate. (**B**) A representative elongated Fe-sulfide particle, located in the dissolution region of the carbonate described in (A), is most likely composed of greigite. The morphology and chemical composition of these particles are similar to the biogenic greigite described in (C). (**C**) High magnification of an individual microorganism within a root cell of a soil sample showing an elongated, multicrystalline core of greigite within an organic envelope.

McKay et al. (1996) figure 6

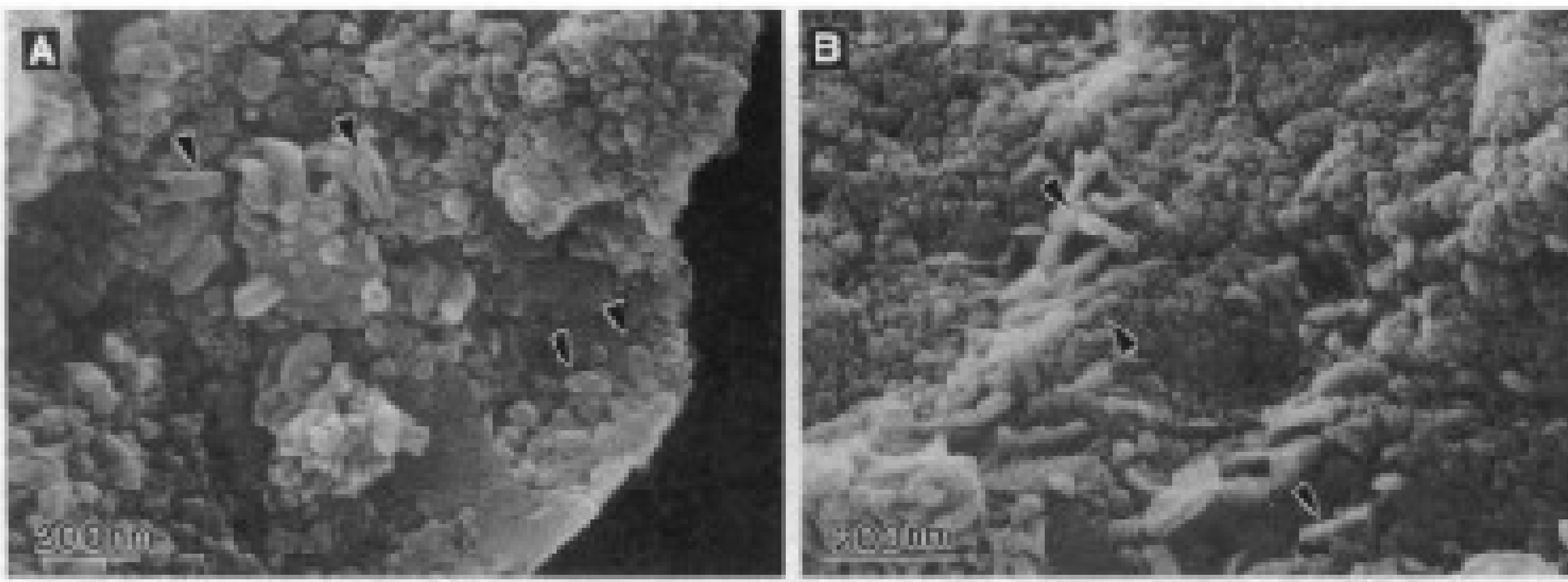

Fig. 6. High-resolution SEM images showing ovoid and elongate features associated with ALH 84001 carbonate globules. **(A)** Surface of Fe-rich rim area. Numerous ovoids, about 100 nm in diameter, are present (arrows). Tubular-shaped bodies are also apparent (arrows). Smaller angular grains may be the magnetite and pyrrhotite found by TEM. **(B)** Close view of central region of carbonate (away from rim areas) showing textured surface and nanometer ovoids and elongated forms (arrows).